Supporting Information

Figure S1

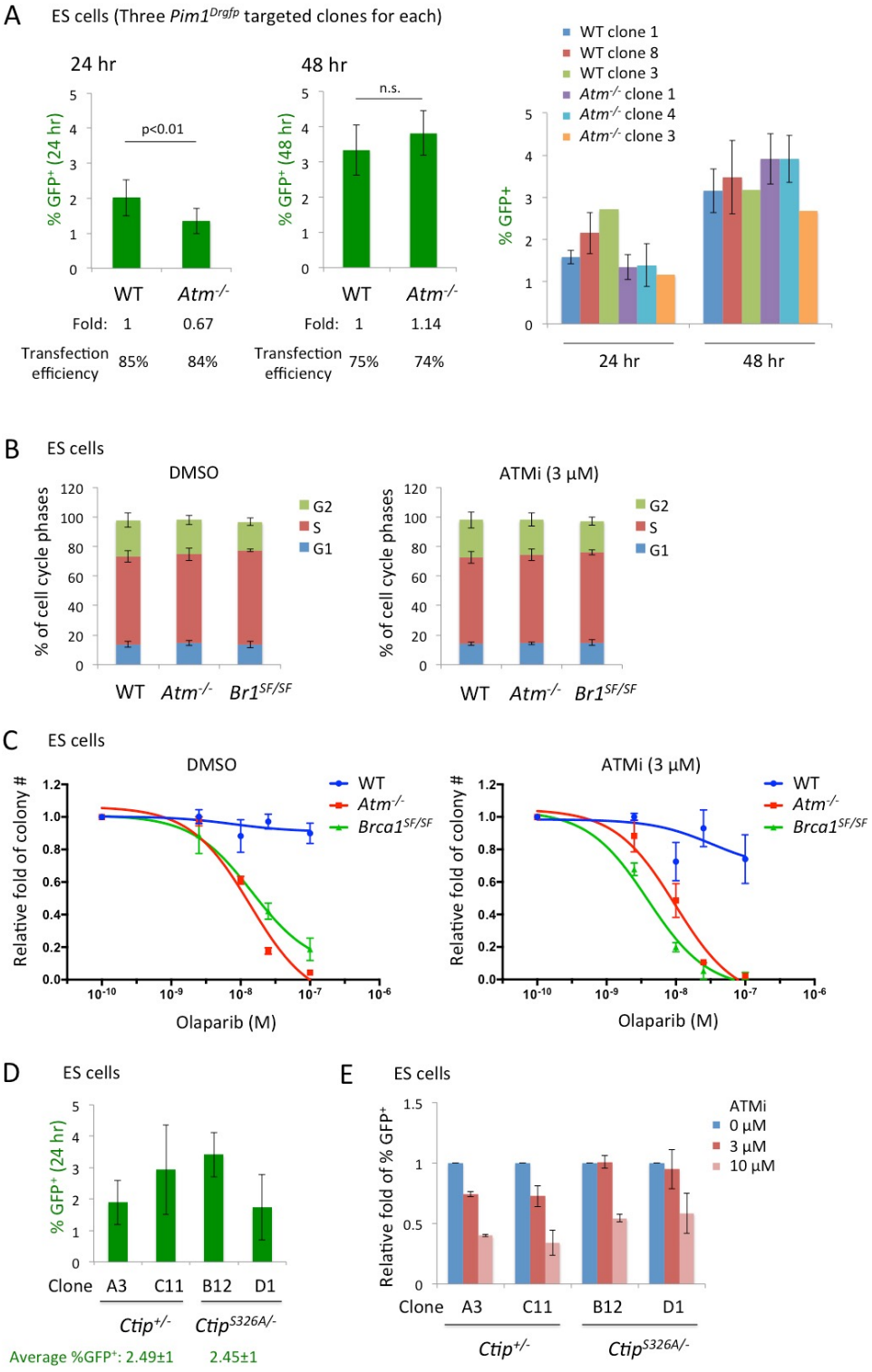

Figure S1

A. Three independent *Pim1*^{Drgfp} targeted clones of WT and *Atm*$^{-/-}$ ES cells, respectively, are examined for HDR activity. The average % GFP^{+} is reduced by ~30% in *Atm*$^{-/-}$ ES cells at 24 hours (left) but not 48 hours (middle) after transfection of an I-SceI expression plasmid, suggesting a delay in HDR. HDR levels of individual clones are summarized (right) and are consistent with the notion above. All error bars in the figures represent one standard deviation from the mean. (WT: n=12; *Atm*$^{-/-}$: n=13 transfections)

B. Treatment of ATMi (3 μM, 24 hours) does not significantly affect cell cycle distribution of ES cells. (n=3)

C. ES cells are transiently treated with different doses of olaparib for 2 days with or without continuous treatment of ATMi (3 μM). IC_{50} of olaparib treatment (2-day pulse) with/without ATMi: *Atm*$^{-/-}$, 13.8/9.8 nM; *Brca1*$^{SF/SF}$, 14.5/3.9 nM.

D. HDR in *Ctip*$^{S326A/-}$ ES cells is not significantly different from *Ctip*$^{+/-}$ cells. Two independent clones are examined for each genotype. (n≥3)

E. ATMi treatment in *Ctip*$^{S326A/-}$ ES cells does not reduce HDR to a greater extent than in the *Ctip*$^{+/-}$ cells. (n≥3)

Figure S2

A E9.5-10.5 (Total: 37) $Atm^{+/-}Brca1^{SF/+}$ x $Atm^{+/-}Brca1^{SF/+}$

Atm	+/+			+/-			-/-		
$Brca1^{SF}$	+/+	SF/+	SF/SF	+/+	SF/+	SF/SF	+/+	SF/+	SF/SF
Observed	4	3	3	4	10	5	2	5	1
Expected	2.3125	4.625	2.3125	4.625	9.25	4.625	2.3125	4.625	2.3125

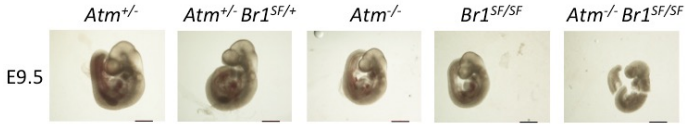

B E12.5-14.5 (Total: 56) $Atm^{+/-}Brca1^{SF/+}$ x $Atm^{+/-}Brca1^{SF/+}$

Atm	+/+			+/-			-/-		
$Brca1^{SF}$	+/+	SF/+	SF/SF	+/+	SF/+	SF/SF	+/+	SF/+	SF/SF
Observed	3	7	3	9	15	8	2	8	1
Expected	3.5	7	3.5	7	14	7	3.5	7	3.5

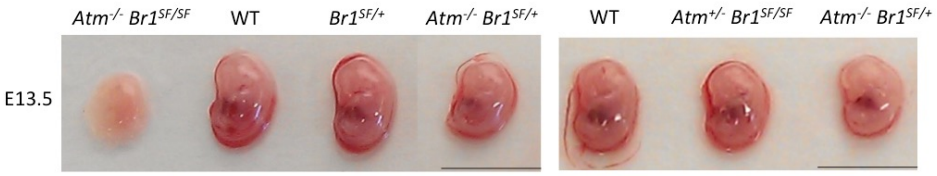

Figure S2
A. One $Atm^{-/-}Brca1^{SF/SF}$ embryo is found at E9.5. The embryo appears slightly smaller than either $Atm^{-/-}$ or $Brca1^{SF/SF}$ single mutant. Scale bar: 1 mm.
B. One $Atm^{-/-}Brca1^{SF/SF}$ embryo is found at E13.5 that is much smaller than other siblings. The MEFs from this embryo fail to plate in culture while MEFs from all other embryos survive. Scale bar: 1 cm.

Figure S3

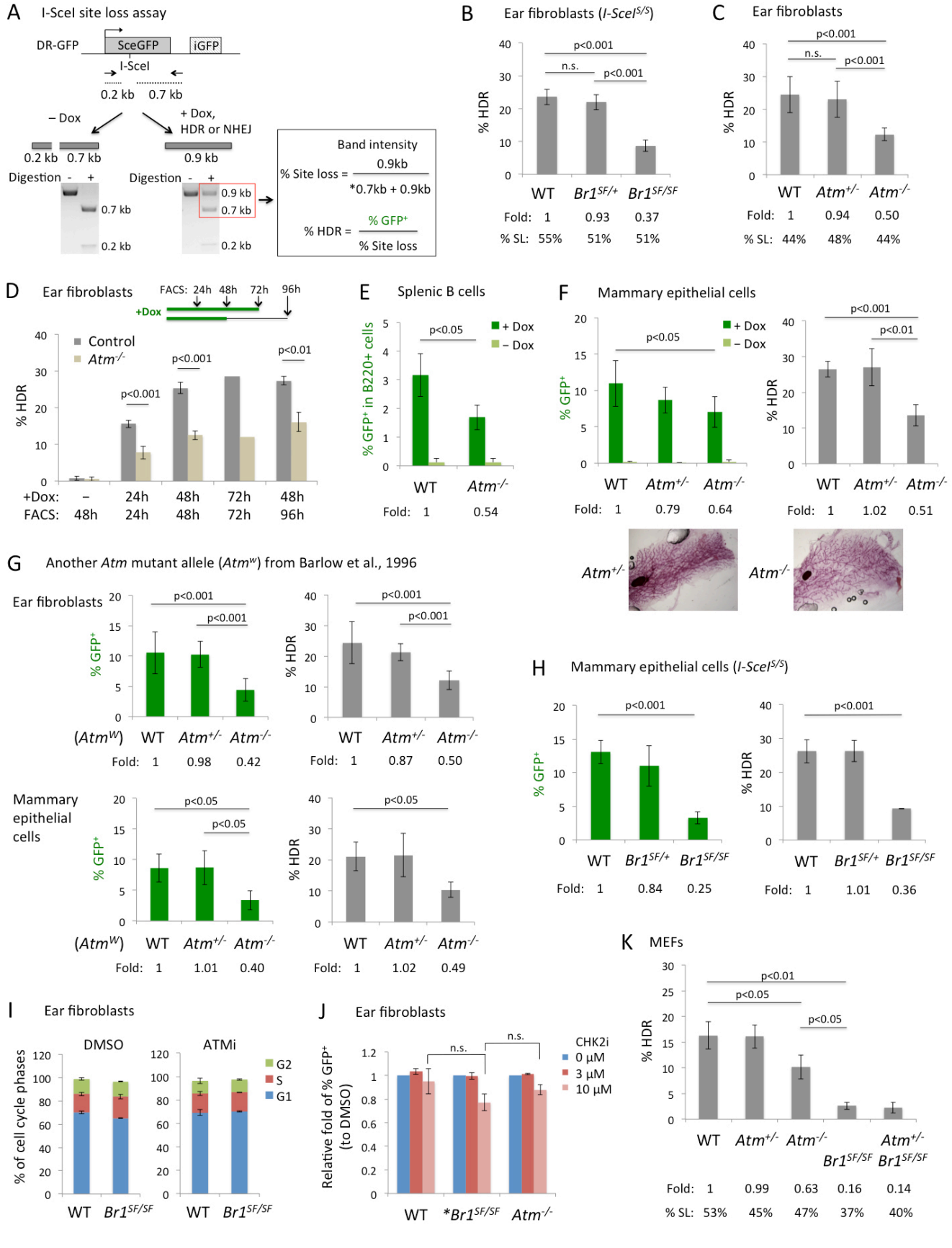
A
I-SceI site loss assay
DR-GFP
SceGFP
iGFP
I-SceI
0.2 kb
0.7 kb
– Dox
+ Dox, HDR or NHEJ
0.9 kb
Digestion
Band intensity
% Site loss = 0.9kb / *0.7kb + 0.9kb
% HDR = % GFP+ / % Site loss
B
Ear fibroblasts (I-SceI S/S)
% HDR
p<0.001
n.s.
WT
Br1 SF/+
Br1 SF/SF
Fold: 1 0.93 0.37
% SL: 55% 51% 51%
C
Ear fibroblasts
% HDR
p<0.001
n.s.
WT
Atm +/-
Atm -/-
Fold: 1 0.94 0.50
% SL: 44% 48% 44%
D
Ear fibroblasts
FACS: 24h 48h 72h 96h
+Dox
Control
Atm -/-
% HDR
p<0.001
p<0.01
+Dox: – 24h 48h 72h 48h
FACS: 48h 24h 48h 72h 96h
E
Splenic B cells
% GFP+ in B220+ cells
p<0.05
+ Dox
– Dox
WT
Atm -/-
Fold: 1 0.54
F
Mammary epithelial cells
% GFP+
p<0.05
+ Dox
– Dox
WT
Atm +/-
Atm -/-
Fold: 1 0.79 0.64
% HDR
p<0.001
p<0.01
Fold: 1 1.02 0.51
Atm +/-
Atm -/-
G
Another Atm mutant allele (Atm W) from Barlow et al., 1996
Ear fibroblasts
% GFP+
% HDR
p<0.001
(Atm W) WT Atm +/- Atm -/-
Fold: 1 0.98 0.42
Fold: 1 0.87 0.50
Mammary epithelial cells
p<0.05
(Atm W) WT Atm +/- Atm -/-
Fold: 1 1.01 0.40
Fold: 1 1.02 0.49
H
Mammary epithelial cells (I-SceI S/S)
% GFP+
% HDR
p<0.001
WT
Br1 SF/+
Br1 SF/SF
Fold: 1 0.84 0.25
Fold: 1 1.01 0.36
I
Ear fibroblasts
DMSO
ATMi
% of cell cycle phases
G2
S
G1
WT
Br1 SF/SF
J
Ear fibroblasts
Relative fold of % GFP+ (to DMSO)
n.s.
CHK2i
0 μM
3 μM
10 μM
WT
*Br1 SF/SF
Atm -/-
K
MEFs
% HDR
p<0.01
p<0.05
WT
Atm +/-
Atm -/-
Br1 SF/SF
Atm +/- Br1 SF/SF
Fold: 1 0.99 0.63 0.16 0.14
% SL: 53% 45% 47% 37% 40%

Figure S3

A. To determine DSB efficiency in the DR-GFP reporter, the sequence flanking the DSB site in the *SceGFP* gene is amplified by primers, followed by *in vitro* digestion with I-SceI endonuclease. Repair of the break by either HDR or imprecise NHEJ results in loss of the I-SceI site, which leaves an intact 0.9-kb product (right gel) in comparison to the digested 0.7- and 0.2-kb bands. This primer set does not amplify SSA products. The % site loss is calculated by dividing the intensity of 0.9-kb band with the sum of 0.9-kb plus 0.7-kb (* accounted for size difference) band. The % HDR, which normalizes % GFP^+ with % site loss, represents the ratio of HDR among total repair events. Dox: doxycycline.

B. Primary ear fibroblasts from *Brca1*$^{SF/SF}$ mice have a ~3-fold reduction in % HDR, consistent with the analysis by % GFP^+. *I-SceI*$^{S/S}$: these mice are homozygous for the *TRE-I-SceI* allele when indicated. (n≥9)

C. Primary ear fibroblasts from *Atm*$^{-/-}$ mice have a ~2-fold reduction in % HDR. (n≥10)

D. Time course of Dox treatment shows that *Atm*$^{-/-}$ fibroblasts consistently have lower HDR than control cells (*Atm*$^{+/-}$ or WT). Cells are exposed to Dox continuously for 24, 48, or 72 hours or for a 48-hour pulse followed by 48-hour recovery to allow time for repair. (n≥3 for all time points except n=1 for 72h)

E. Primary splenic B cells from *Atm*$^{-/-}$ mice have a 2-fold reduction in HDR. The % GFP^+ is measured from the purified $B220^+$ B cells stimulated with LPS and IL4. (n=3)

F. Primary mammary epithelial cells harvested from *Atm*$^{-/-}$ mice have a ~2-fold reduction in HDR. Mammary gland from a 12-week-old *Atm*$^{-/-}$ mouse shows relatively normal elongation of ductal trees that fill the fat pad, albeit with less secondary branching compared to the littermate control (bottom). (n≥4)

G. All the *Atm* experiments in the paper are performed with the *Atm* mutant allele with the exons encoding the kinase domain deleted (1). For comparison, another strain of *Atm* mutant mice (*Atm*^{w}) is examined. *Atm*^{w} allele contains an exon deletion upstream of the kinase domain (2). Primary ear fibroblasts and mammary cells harvested from the *Atm*^{w} mutant mice show a consistent 2-fold reduction in HDR. (n≥3)

H. Primary mammary epithelial cells from *Brca1*$^{SF/SF}$ mutant mice have a ~3-fold reduction in % HDR. (n≥3)

I. Cell cycle profiles show no significant difference between WT and *Brca1*$^{SF/SF}$ primary ear fibroblasts following ATMi treatment (3 μM). Note that these cells are from +Dox 48-hour treatment and thus have higher G1 vs. S/G2 ratio than the profiles in Fig. S4H. (n=2)

J. Inhibition of CHK2 slightly reduces HDR in *Brca1*$^{SF/SF}$ ear fibroblasts, but the extent is not significantly different from that of WT or *Atm*$^{-/-}$ cells. * *Brca1*$^{SF/SF}$: *Atm*$^{+/+}$ or *Atm*$^{+/-}$ (n=3 for WT and *Brca1*$^{SF/SF}$, n=2 for *Atm*$^{-/-}$)

K. *Brca1*$^{SF/SF}$ primary MEFs show a substantial reduction in % HDR (~6-fold) compared to WT MEFs, while the reduction in *Atm*$^{-/-}$ MEFs is less profound (~1.5-fold). (n≥3 except n=2 for *Brca1*$^{SF/SF}$)

Additional notes on the site loss assay. The HDR reduction we observed in *Atm* mutant cells was surprising, given that reports from several labs have not uncovered an essential role for ATM in HDR. In particular, we previously did not detect a significant defect in HDR in *Atm*$^{-/-}$ primary mouse fibroblasts (3). Previous experiments have relied on transient transfection of an I-SceI expression vector, which in primary cells is variable and relatively inefficient (~20%), such that the fraction of DSB repair events that involved HDR could not be determined. Dox-inducible I-SceI expression, by contrast, results in DSB formation in a substantially higher percentage of cells (4). This allows us to normalize HDR levels to total repair events to determine the percentage of cells that had repaired the DSB by either HDR or imprecise NHEJ (Fig. S3A).

The site loss for WT and *Atm*$^{-/-}$ ear fibroblasts was similar (44% for each) (Fig. S3C), as it was for MEFs (53% and 47%, respectively; Fig. S3K), indicating that the DSB efficiency and total repair was similar for both genotypes. The fraction of HDR among total repair events (i.e. % HDR) was estimated to be 25% for WT and 12% for *Atm*$^{-/-}$ ear fibroblasts, confirming that loss of ATM reduces HDR by 2-fold in this assay. HDR was also confirmed by the site loss assay to be reduced in *Atm*$^{-/-}$ MEFs to a lesser extent than in ear fibroblasts (Fig. S3 C and K), while the *Brca1*$^{SF/SF}$ cells showed the converse in that HDR was reduced to a greater extent in MEFs than in ear fibroblasts (Fig. S3 B and K).

Site loss assays to determine % HDR were also performed for ATMi-treated cells, results of which are presented in the Supporting Data File. In this case, cells from the same animal are treated with DMSO or ATMi, and so are internally controlled. The ratios of ATMi vs. DMSO using the normalized % HDR values are consistent with the analysis using % GFP^+.

Figure S4

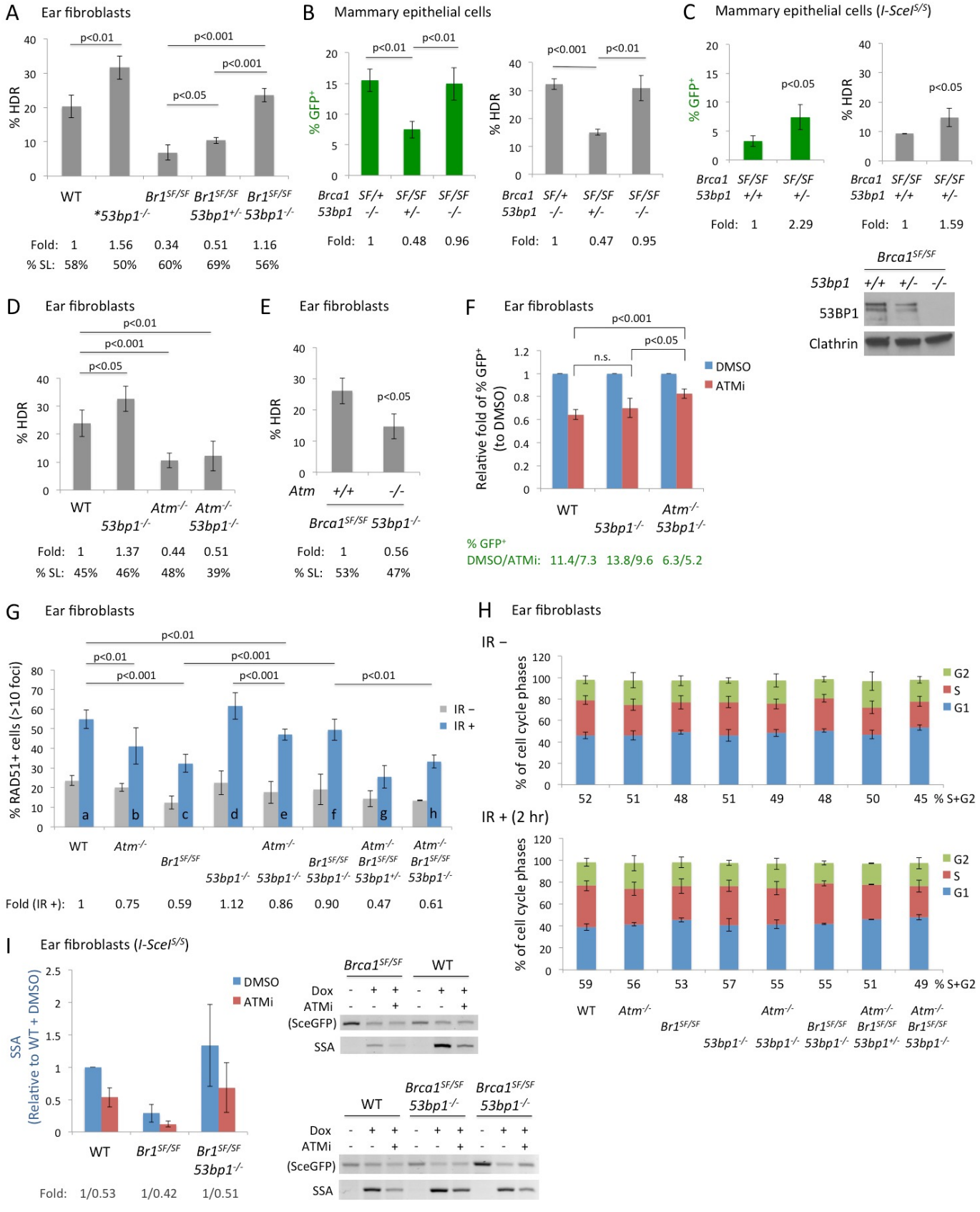
A
Ear fibroblasts
% HDR
WT
*53bp1-/-
Br1SF/SF
Br1SF/SF 53bp1+/-
Br1SF/SF 53bp1-/-
Fold: 1 1.56 0.34 0.51 1.16
% SL: 58% 50% 60% 69% 56%
B
Mammary epithelial cells
% GFP+
% HDR
Brca1 53bp1
SF/+ -/-
SF/SF +/-
SF/SF -/-
Fold: 1 0.48 0.96
Fold: 1 0.47 0.95
C
Mammary epithelial cells (I-SceIS/S)
% GFP+
% HDR
Brca1 53bp1
SF/SF +/+
SF/SF +/-
Fold: 1 2.29
Fold: 1 1.59
Brca1SF/SF
53bp1 +/+ +/- -/-
53BP1
Clathrin
D
Ear fibroblasts
% HDR
WT
53bp1-/-
Atm-/-
Atm-/- 53bp1-/-
Fold: 1 1.37 0.44 0.51
% SL: 45% 46% 48% 39%
E
Ear fibroblasts
% HDR
Atm +/+ -/-
Brca1SF/SF 53bp1-/-
Fold: 1 0.56
% SL: 53% 47%
F
Ear fibroblasts
Relative fold of % GFP+ (to DMSO)
DMSO
ATMi
n.s.
WT
53bp1-/-
Atm-/- 53bp1-/-
% GFP+
DMSO/ATMi: 11.4/7.3 13.8/9.6 6.3/5.2
G
Ear fibroblasts
% RAD51+ cells (>10 foci)
IR –
IR +
WT
Atm-/-
Br1SF/SF
53bp1-/-
Atm-/- 53bp1-/-
Br1SF/SF 53bp1+/-
Fold (IR +): 1 0.75 0.59 1.12 0.86 0.90 0.47 0.61
H
Ear fibroblasts
IR –
IR + (2 hr)
% of cell cycle phases
G2
S
G1
52 51 48 51 49 48 50 45 % S+G2
59 56 53 57 55 55 51 49 % S+G2
WT
Atm-/-
Br1SF/SF
53bp1-/-
Atm-/- 53bp1-/-
Br1SF/SF 53bp1+/-
I
Ear fibroblasts (I-SceIS/S)
SSA (Relative to WT + DMSO)
DMSO
ATMi
WT
Br1SF/SF
Br1SF/SF 53bp1-/-
Fold: 1/0.53 1/0.42 1/0.51
Brca1SF/SF
WT
Dox
ATMi
(SceGFP)
SSA
Brca1SF/SF 53bp1-/-
Brca1SF/SF 53bp1-/-

Figure S4

A. Homozygous deletion of *53bp1* restores the levels of % HDR in *Brca1*$^{SF/SF}$ ear fibroblasts. Heterozygous deletion of *53bp1* in *Brca1*$^{SF/SF}$ ear fibroblasts also increases % HDR by ~50%. **53bp1*$^{-/-}$: *Brca1*$^{+/+}$ or *Brca1*$^{SF/+}$ (n≥3 except n=2 for *53bp1*$^{-/-}$)

B. Homozygous deletion of *53bp1* also restores HDR in *Brca1*$^{SF/SF}$ mammary epithelial cells. (n≥3)

C. Heterozygous deletion of *53bp1* significantly increases HDR in *Brca1*$^{SF/SF}$ mammary epithelial cells. The level of 53BP1 protein is attenuated in *53bp1*$^{+/-}$ compared to *53bp1*$^{+/+}$ mammary cells. (n≥3)

D. Loss of *53bp1* does not rescue the reduction in % HDR in *Atm*$^{-/-}$ ear fibroblasts. (n≥4)

E. Loss of *Atm* in *Brca1*$^{SF/SF}$*53bp1*$^{-/-}$ ear fibroblasts still decreases % HDR. (n=4 for *Brca1*$^{SF/SF}$*53bp1*$^{-/-}$; n=2 for triple mutant)

F. ATMi (3 μM) treatment reduces HDR in *53bp1*$^{-/-}$ ear fibroblasts to a similar extent as in WT cells. (n≥5)

G. Loss of *Atm* in *Brca1*$^{SF/SF}$*53bp1*$^{-/-}$ ear fibroblasts reduces % RAD51^{+} cells following ionizing radiation (IR). Primary ear fibroblasts (passage 1) are plated overnight, treated with or without 10 Gy IR, and allowed for recovery for 2 hours. The analysis is performed from at least three animals (for IR + samples), each with ~200 total cells counted.

H. Cell cycle profiles show no apparent difference between WT and mutant fibroblasts 2 hours after 10 Gy IR (i.e., the same treatment for staining of DNA damage foci).

I. While loss of *53bp1* rescues the SSA defect in *Brca1*$^{SF/SF}$ ear fibroblasts, treatment of ATMi still reduces SSA in *Brca1*$^{SF/SF}$*53bp1*$^{-/-}$ cells by ~2-fold as in WT cells. (n≥3)

Supporting Materials and Methods

Mouse genotyping

Genomic DNA was extracted from tail tips using Gentra Puregene Mouse Tail Kit (Qiagen). PCR reactions were performed with PuReTaq PCRbeads (GE Healthcare). Genotyping protocols were as described for *Atm*^{b}, *Atm*^{w}, and *Pim1*^{Drgfp} (3) and *TRE-I-SceI* mice. *Brca1*^{S1598F} mice (5) were genotyped using primers S1598F.for 5'-CCC TTG TGC ACC TCC AGA GA-3'; S1598F.rev 5'-GCC ACG CCT ATG AAG GCT CT-3' and LNL3xpA 5'-GAC CTG CAG CCC AAG CTA GC-3' under the following conditions: 94°C/3 min; 35 cycles of 94°C/30 sec, 58°C/30 sec and 72°C/1 min; and a final extension of 72°C/5 min. PCR products (Wild-type: 259 bp; Mutant: 117 bp) were separated on a 2% agarose gel. *53bp1* mice (6) were genotyped using primers exon4 sense 5'-GAT TTT GCC TTA CCC AGT TCC CGA-3'; neo sense 5'-CTA CCC GGT AGA ATT GAC CTG CA-3' and intron antisense 5'-CCT TCT ATT CTA CTT CAG GCT CTG G-3' under the following conditions: 94°C/4 min; 40 cycles of 94°C/30 sec, 55°C/1 min and 72°C/1 min; and a final extension of 72°C/5 min. PCR products (Wild-type: ~300 bp; Mutant: ~200 bp) were separated on a 2% agarose gel. *Chk2* mice (7) were genotyped using primers WT#1F 5'-GTG TGC GCC ACC ACT ATC CTG-3'; WT#2R 5'-CCC TTG GCC ATG TTT CAT CTG-3' and Neop53 5'-TCC TCG TGC TTT ACG GTA TC-3' following the same condition as the *Brca1*^{S1598F} genotyping PCR (Wild-type: 439 bp; Mutant: ~600 bp).

Primary cell cultures

All experimental mice were hemizygous for the *Pim1*^{drgfp} and *CMV-rtTA* alleles. The *TRE-I-SceI* allele was also hemizygous, except when labeled as *I-SceI*$^{S/S}$ to indicate homozygous alleles; no significant difference in % GFP^{+} between hemizygous and homozygous *TRE-I-SceI* alleles was observed in HDR assays.

Primary ear fibroblasts and MEFs were cultured in DMEM-HG medium supplemented with 10% tetracycline-free FBS (Clontech), 1X Pen-Strep, and 1X MEM/NEAA. Primary mammary epithelial cells were cultured in DMEM-HG:F12 medium with 10% tetracycline-free FBS, 1X Pen-Strep, 10 μg/ml insulin and 5 ng/ml EGF.

For ear fibroblast isolation, ear tips are cut from 6- to 8-week-old mice, minced with a razor blade, and dissociated in 5 ml serum-free DMEM medium containing 2 mg/ml collagenase A (Roche) and 1X Pen-Strep on a 37°C shaker for 3 hr. The dissociated tissues were passed through a 70-μm strainer, pelleted by centrifugation at 400 g for 8 min, and plated to 6-well plate for 1-2 days before experiments.

For MEF isolation, E12.5-E14.5 mouse embryos were separated from the placenta and embryonic sac, then minced following the removal of head and liver, and then dissociated in 0.05% trypsin at 37°C for 45 min in a 6-cm dish. The dissociated cells were resuspended by pipetting, pelleted at 400 g for 10 min, and plated to a 6-cm dish coated with 0.1% gelatin for 1-2 days.

For mammary epithelial cell isolation, the 4th inguinal mammary glands from 8- to 10-week-old virgin female mice were minced and dissociated in 5 ml serum-free DMEM-HG:F12 containing 2 mg/ml collagenase A, 5 μg/ml insulin, and 1X Pen-Strep on a 37°C shaker for 2 hr. The dissociated cells were pelleted at 400 g for 10 min, resuspended in 6 ml serum-free DMEM-HG:F12 containing 10 μg/ml DNase I (Stem Cell Technologies) and inverted for 2 min, and then pelleted again by centrifugation. Red blood cells were lysed with ammonium chloride solution (Stem Cell Technologies), and the epithelial organoids were separated from other cell types using two sequential short spins (10 and 5 sec) at 400 g, and then plated to 6-well plate coated with collagen I for 1 day.

For HDR assays, primary fibroblasts and mammary epithelial cells at passage one were plated at a density of 10^5 cells per single well of 6-well plate the night before, then treated with 1 μg/ml Dox (Clontech) to induce I-SceI expression. The percentage of GFP^{+} cells was analyzed after 48 hr by flow cytometry. For inhibition of ATM, 3 μM KU-55933 (Calbiochem #118502, 10 mM solution) or equal volume of DMSO were added together with Dox and replenished at 24 hr. For CHK2 inhibition (EMD Millipore #220486), the same procedure is followed.

Primary B cells were purified from mouse spleens by CD43 negative selection (Miltenyi Biotec 130-049-801) as described (8). The B cells were cultured at a density of 10^6 cells/ml, stimulated with cytokines (10 μg/ml LPS, 2 μg/ml anti-CD40, and 25 μg/ml mouse IL4) in combination with 0.25 μg/ml Dox. The B220^{+}GFP^{+} cells were analyzed by flow cytometry at 96 hr.

Mouse ES cell culture and transfection

Brca1$^{SF/SF}$ DR-GFP mouse ES cell lines have been previously described (5). *Atm*$^{-/-}$ ES cells (1) and WT J1 ES cells were targeted with a linearized DR-GFP plasmid to the *Pim1* locus (9). All mouse ES cell lines were cultured in DMEM-HG medium supplemented with 12.5% stem cell grade FBS (Gemini), 1X Pen-Strep, 1X MEM/NEAA, 1X L-Gln, 833 U/ml LIF (Gemini), and 0.1 mM β-mercaptoethanol. Culture dishes were pre-coated with 0.1% gelatin. For electroporation, 3-4 × 10^6 ES cells per 10-cm dish were plated the night before. Typically a total of 3 × 10^6 cells and 30 μg plasmid DNA were used for each reaction. The trypsinized cells were resuspended in 600 μl Opti-MEM, mixed with plasmids, and pulsed with a Gene Pulser Xcell (Bio-Rad) in a 0.4 cm cuvette at 250 V/950 μF. After pulsing, the cells were mixed with growth medium and plated to a 6-cm dish; for ATM inhibition, the transfection mixture was split to two wells of a 6-well plate

containing ATMi KU-55933 or an equal volume of DMSO, replenished at 24 hr. As a control for transfection efficiency, a pNZ-EGFP plasmid and a pCAGGS empty vector were transfected in independent reactions, respectively.

Site-loss PCR assays

Genomic DNA was extracted from primary cells following I-SceI induction using Gentra Puregene Mouse Tail Kit (Qiagen). The sequence spanning the I-SceI cleavage site in the *SceGFP* gene was amplified from 100 ng of genomic DNA using Advantage 2 Polymerase (Clontech) with forward primer dr.for 5'-CCC GCC ACC TGC CCC ATC TGC TA-3' and reverse primer dr.rev 5' -CCT CTA CAA ATG TGG TAT GGC TGA TTA TG-3'; this primer set does not amplify SSA products. The PCR condition is as follows: 95°C/1 min; 33 cycles of 95°C/15 sec and 70°C/2 min; and a final extension of 70°C/5 min. The PCR products were aliquoted in half and digested with 8 U I-SceI endonuclease (Thermo Fisher Scientific) or buffer-only control *in vitro* at 37°C overnight and separated on a 1% agarose gel. Band intensities were quantified using ImageJ. The intensity of the uncut band (0.9 kb) was divided by the sum of the uncut (0.9 kb) plus the large cut band (0.7 kb; accounted for the size difference with a correction factor) to calculate % I-SceI site loss.

SSA PCR

SSA analysis was performed as described (10). Briefly, the products of SSA were amplified from 200 ng genomic DNA extracted from primary cells following I-SceI induction using PuReTaq PCR beads (GE Healthcare) with forward primer SA.F 5'-TTT GGC AAA GAA TTC AGA TCC-3' and reverse primer SA.R2 5'-ATG ACC ATG ATT ACG CCA AG-3'. For comparison, the structurally intact *SceGFP* gene (or one that had undergone HDR or NHEJ) was amplified using the same forward primer and a different reverse primer SA.R1 5'-CAA ATG TGG TAT GGC TGA TTA TG-3' from 100 ng genomic DNA. The band intensity of SSA product (0.9 kb) was normalized to that of SceGFP (1.1 kb) for each sample, and a relative fold was derived between mutant and control samples on the same gel.

Cell cycle analysis

Trypsinized cells were resuspended in 300 µl ice-cold PBS, and 700 µl of ice-cold 100% ethanol was added drop-wise to the cells while vortexing at low speed to a final concentration of 70% ethanol. The samples were fixed at -20°C at least overnight, then pelleted at 2000 g for 5 min, washed with PBS once, and incubated in 200 µl staining solution (25 µg/ml propidium iodide, 0.1 mg/ml RNase A, 0.05% Triton X-100 in PBS) at 37°C for 30 min followed by flow cytometry. The cell cycle distribution was analyzed using FlowJo cell cycle analysis tool.

Colony formation assay

Mouse ES cells were plated at a density of 1200 cells per well in 6-well plates overnight. Cells were pre-treated with 3 µM ATMi KU-55933 or DMSO for 2 hr, and then treated with PARPi olaparib (synthesized in the MSKCC Organic chemistry core facility) in combination with ATMi or DMSO for 48 hr. After removing the olaparib-containing medium, the cells were gently washed with PBS once and then incubated with medium containing only ATMi or DMSO for another 3-4 days until colonies become visible. The colonies were fixed in 100% methanol for 20 min and then stained in 3% Giemsa for 3-4 hr. IC_{50} is plotted by nonlinear regression using Prism 6 software.

Mammary gland whole mount staining

The 4th inguinal mammary glands from >8-week-old virgin female mice were harvested and gently spread on microscope slides with a sheet of parafilm. The slides were fixed in Carnoy's fixative (60% ethanol, 30% chloroform, and 10% glacial acetic acid) overnight, defatted in acetone for 30 min, sequentially washed in 70%/50%/30% ethanol for 15 min each and in distilled water for 5 min. The rehydrated slides were incubated in carmine alum solution (2% carmine, 5% aluminum potassium sulfate in water) at room temperature (RT) overnight. After staining, the slides were dehydrated with sequential washes in 70%/95%/100% ethanol for 15 min each, incubated in fresh 100% ethanol for 15 min, cleared in CitriSolv (Fisher Scientific) overnight until the fat pads become transparent, and sealed in Permount mounting medium (Fisher Scientific) for photography.

Western blotting

Proliferating cells were scraped from dishes on ice and lysed for 30 min on ice in 10 mM Tris, pH 8, 1 mM EDTA, 10% glycerol, 0.5% NP-40, and 400 mM NaCl with freshly added 1 mM DTT and 1X protease/phosphatase inhibitor EDTA-free cocktails (Pierce). Lysates were centrifuged at 13000 g for 20 min and the supernatant was collected. Protein concentration was quantified using Bradford protein assay (Bio-Rad). 53BP1 was separated on 3-8% Tris-Acetate gels (Invitrogen) and transferred to a PVDF membrane in Tris-Glycine buffer containing 0.01% SDS and 10% methanol at 22V, 4°C overnight. Blocking was performed in 5% milk diluted in PBST (1X PBS/0.1% Tween-20) at RT for 1 hr. Primary antibodies were diluted in 2.5% milk and incubated at 4°C overnight on a rotator. HRP-conjugated secondary antibodies (GE Healthcare) were diluted 1:10000 in 2.5% milk and incubated at RT for 1 hr on a shaker. Each incubation was followed by three 10

min-washes in PBST. The membranes were developed using Enhanced ECL reagents (PerkinElmer). Primary antibodies used: Anti-53BP1: 1:4000 (Novus NB100-304); Anti-Clathrin heavy chain: 1:10000 (BD Biosciences 610500).

Immunofluorescence staining

Primary ear fibroblasts were plated in 8-well chamber slides (BD Falcon; pre-coated with poly-L-lysine) at a density of 2×10^4 cells per well overnight, followed by 10 Gy IR and 2 hr recovery. Cells were fixed in fresh 3% paraformaldehyde/2% sucrose/PBS at RT for 10 min. After fixing, the slides are washed with PBS once, permeabilized in 0.5% Triton X-100/PBS at RT for 10 min, and blocked in 1% IgG-free BSA (Jackson ImmunoResearch)/0.1% Triton X-100/PBS on a shaker at RT for 30 min. The slides were incubated with primary and secondary antibodies diluted in blocking buffer (70 μl/well) at RT on a shaker for 2 and 1 hr, respectively. Following each staining step the slides were washed with PBS 3x, 10 min each on a shaker. Finally, the slides were fixed in ProLong Gold Antifade Mountant with DAPI (Molecular Probes) and analyzed by microscopy. Antibodies used: Anti-RAD51: 1:400 (Calbiochem PC130). Alexa Fluor 488/594-conjugated secondary antibodies: 1:400 (Molecular Probes).

Supporting References

1. Xu Y & Baltimore D (1996) Dual roles of ATM in the cellular response to radiation and in cell growth control. *Genes Dev.* 10(19):2401-2410.
2. Barlow C*, et al.* (1996) Atm-deficient mice: a paradigm of ataxia telangiectasia. *Cell* 86(1):159-171.
3. Kass EM*, et al.* (2013) Double-strand break repair by homologous recombination in primary mouse somatic cells requires BRCA1 but not the ATM kinase. *Proc. Natl. Acad. Sci. U. S. A.* 110(14):5564-5569.
4. Kass EM, Lim PX, Helgadottir HR, Moynahan ME, & Jasin M (2016) Robust homology-directed repair within mouse mammary tissue is not specifically affected by Brca2 mutation. *Nat Commun* 7:13241.
5. Shakya R*, et al.* (2011) BRCA1 tumor suppression depends on BRCT phosphoprotein binding, but not its E3 ligase activity. *Science* 334(6055):525-528.
6. Ward IM, Minn K, van Deursen J, & Chen J (2003) p53 Binding protein 53BP1 is required for DNA damage responses and tumor suppression in mice. *Mol. Cell. Biol.* 23(7):2556-2563.
7. Hirao A*, et al.* (2002) Chk2 is a tumor suppressor that regulates apoptosis in both an ataxia telangiectasia mutated (ATM)-dependent and an ATM-independent manner. *Mol. Cell. Biol.* 22(18):6521-6532.
8. Zheng S*, et al.* (2015) Non-coding RNA Generated following Lariat Debranching Mediates Targeting of AID to DNA. *Cell* 161(4):762-773.
9. Moynahan ME, Pierce AJ, & Jasin M (2001) BRCA2 is required for homology-directed repair of chromosomal breaks. *Mol. Cell* 7(2):263-272.
10. Nakanishi K*, et al.* (2005) Human Fanconi anemia monoubiquitination pathway promotes homologous DNA repair. *Proc. Natl. Acad. Sci. U. S. A.* 102(4):1110-1115.